Ecological Applications, 26(8), 2016, pp. 2623–2636

Aggregation and a strong Allee effect in a cooperative outbreak insect

D. W. Goodsman,[1,5] D. Koch,[2] C. Whitehouse,[3] M. L. Evenden,[1] B. J. Cooke,[4] and M. A. Lewis[1,2]

[1]*Department of Biological Sciences, University of Alberta, CW 405, Biological Sciences Bldg, Edmonton, Alberta T6G 2E9 Canada*
[2]*Mathematical and Statistical Sciences, University of Alberta, 632 CAB, Edmonton, Alberta T6G 2G1 Canada*
[3]*Operations Division, Alberta Agriculture and Forestry, Peace River, Alberta T8S 1T4 Canada*
[4]*Canadian Forest Service, Northern Forestry Centre, 5320 122 Street Northwest, Edmonton, Alberta T6H 3S5 Canada*

Abstract. Most species that are negatively impacted when their densities are low aggregate to minimize this effect. Aggregation has the potential to change how Allee effects are expressed at the population level. We studied the interplay between aggregation and Allee effects in the mountain pine beetle (*Dendroctonus ponderosae* Hopkins), an irruptive bark beetle that aggregates to overcome tree defenses. By cooperating to surpass a critical number of attacks per tree, the mountain pine beetle is able to breach host defenses, oviposit, and reproduce. Mountain pine beetles and Hymenopteran parasitoids share some biological features, the most notable of which is obligatory host death as a consequence of parasitoid attack and development. We developed spatiotemporal models of mountain pine beetle dynamics that were based on the Nicholson–Bailey framework but which featured beetle aggregation and a tree-level attack threshold. By fitting our models to data from a local mountain pine beetle outbreak, we demonstrate that due to aggregation, attack thresholds at the tree level can be overcome by a surprisingly low ratio of beetles per susceptible tree at the stand level. This results confirms the importance of considering aggregation in models of organisms that are subject to strong Allee effects.

Key words: Allee; Dendroctonus ponderosae *Hopkins; dispersal; insect; integrodifference; management; model; mountain pine beetle; outbreak; parasitoid; population dynamics.*

Introduction

Allee effects, in which the fitness of individuals increases with the density or number of conspecifics (Allee 1931, Stephens et al. 1999), underlie irruptive dynamics in many insects (Heavilin and Powell 2008, Liebhold and Tobin 2008). These can be further subdivided into strong Allee effects, characterized by the presence of an extinction threshold, and weak Allee effects, which lack such a threshold (Courchamp et al. 2008). Strong Allee effects can be exploited by managers to control pest species because populations need only be pushed below the strong Allee threshold to ensure extirpation (Liebhold and Tobin 2008, Tobin et al. 2011). Dispersal can also increase the extinction-proneness of populations impacted by strong Allee effects, because it decreases population density, which can push populations below extinction thresholds (Taylor and Hastings 2005, Robinet et al. 2008). Thus, dispersal and Allee effects are interconnected and an adequate representation of dispersal is required to predict the impacts of strong Allee thresholds on populations.

Many dispersing organisms that are impacted by Allee effects, however, have evolved mechanisms that enable aggregation in order to avoid extinction (Gascoigne et al. 2009). Aggregation may ensure population persistence even under heavy management or wide dispersal. Due to dispersal and aggregation, Allee effects that are expressed at the individual level (Courchamp et al. 2008) may not translate directly to demographic Allee effects observable at the population level. It is therefore important to understand how Allee thresholds, dispersal, and aggregation interact.

The mountain pine beetle (*Dendroctonus ponderosae* Hopkins) system is ideal for exploring interactions between dispersal, aggregation, and Allee effects. In the late summer, beetles disperse locally underneath the canopy in search of new host trees (Safranyik et al. 1992), but they also immigrate due to long-distance dispersal via the atmospheric boundary layer (Jackson et al. 2008). After dispersing, female mountain pine beetles lead the attack by flying to potential host trees and chewing through their bark. Trees respond to attacking female beetles by exuding resin laden with defense chemicals. Chemicals in the resin interact synergistically with pheromones released by female beetles to draw in other beetles to help with the attack (Conn et al. 1983). By mass-attacking, beetles are sometimes able to subdue trees sufficiently to begin excavating galleries without being pitched out of entrance holes by resin flow (Raffa and Berryman 1983, Boone et al. 2011). If, however, the

Manuscript received 9 November 2015; revised 21 April 2016; accepted 13 June 2016. Corresponding Editor: M. P. Ayres.
[5]E-mail: goodsman@ualberta.ca

number of attacking beetles in the mass-attack is insufficient, beetles will be pitched out or killed inside the tree (Raffa and Berryman 1983). Thus, tree defenses lead to a highly nonlinear strong Allee relationship governing beetle attack success at the individual tree-level (Boone et al. 2011).

There are phenomenological Allee effect models of the mountain pine beetle system (Heavilin and Powell 2008) which contain minimal biological detail, but also some mechanistic models that have incorporated pheromone communication and aggregation (Biesinger et al. 2000, Strohm et al. 2013). Detailed mechanistic models such as these are complex and difficult to simulate and fit to data. On the other hand, the use of simple phenomenological models that do not account for dispersal, aggregation, and immigration may give managers false confidence in population suppression strategies.

To explore the interplay between dispersal, aggregation, and Allee effects, we constructed integrodifference equation models of mountain pine beetle dynamics based on the Nicholson–Bailey framework (Nicholson 1933, Nicholson and Bailey 1935). Nicholson–Bailey models typically represent the population dynamics of Hymenopteran parasitoids and their hosts (Hassell 1978). Parasitoids are distinguished from parasites because they kill their host in order to develop, a trait they share with mountain pine beetles. Nicholson–Bailey models in their original form, however, are not appropriate for mountain pine beetle–tree systems because many mountain pine beetles emerge from a single host tree, which succumbs to attack only if a critical number of attacks is surpassed through aggregation (Raffa and Berryman 1983).

The attack threshold may result in a demographic Allee threshold at the stand level such that the mountain pine beetle population grows if it is above the Allee threshold and goes extinct otherwise. The demographic Allee threshold will equal the attack threshold (measured in beetles/tree) if a mountain pine beetle population spreads attacks evenly among all susceptible host trees in the stand. In this unrealistic scenario, either all trees in the stand will be successfully attacked or none will. Because mountain pine beetles are known to aggregate their attacks (Raffa and Berryman 1983), we hypothesized that the ratio of beetles/susceptible tree required to overcome the demographic Allee threshold would be considerably smaller than number of beetles required to kill a single tree (Fig. 1). We fitted our models to data to estimate aggregation and threshold parameters and to gain insight into how they impact mountain pine beetle dynamics.

Data

An objective of this modeling study was to synthesize biologically relevant data on the location and density of attacked trees, forest stand inventory, and mountain pine beetle productivity.

Study area and infested tree data

The mountain pine beetle attacks trees in the summer, but foliage of successfully attacked trees typically takes a year to turn from green to red. Red attacked trees can be detected by aerial surveyors, whereas recently attacked green trees must be discovered and confirmed with ground surveys. Our infestation data were recorded by aerial surveyors as point data that represented the centre of clusters of between one and 30 red attacked trees.

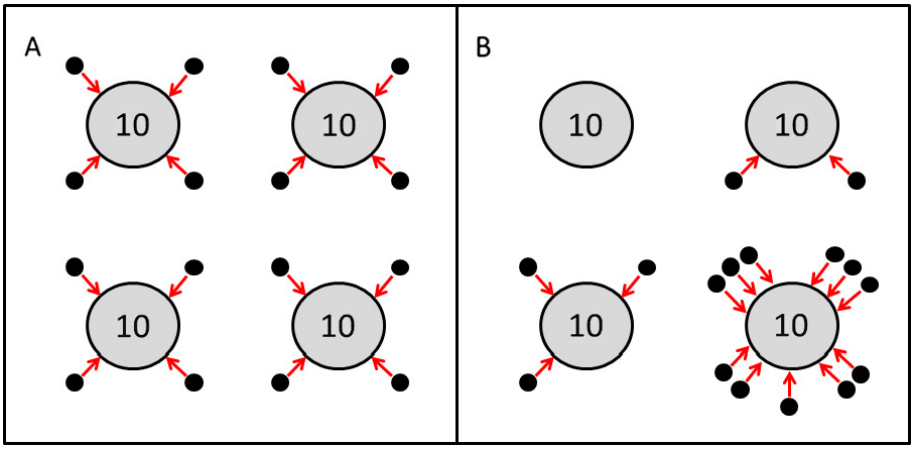

Fig. 1. A graphical depiction of a hypothesis that describes how aggregation changes the way in which host attack thresholds scale up to the population level. In a hypothetical host in which the number of parasitoid attacks required for attack is 10 attacks per host (large gray circles) and in which each parasitoid (small black circles) can only attack a single host. No hosts can be colonized (A) in the absence of aggregation if there are a total of 16 parasitoids and four hosts in the population because the parasitoids distribute their attacks evenly among the hosts. However, (B) with aggregation, the same ratio of parasitoids to hosts can result in one host being successfully colonized. In fact, if aggregation is extreme such that all parasitoids attack a single host, the population level threshold for one host to be successfully attacked is 10 parasitoids divided by four hosts (2.5 parasitoids per host), a number much smaller than the host-level threshold for successful attack of 10 attacks per host.

To obtain data that represent natural mountain pine beetle dispersal and infestation processes, we selected a study region inside Willmore Wilderness Park, a park where no motorized vehicle access or commercial forestry activity is permitted (Fig. 2A). Willmore Wilderness Park borders British Columbia, Canada, and is located in the Rocky Mountain natural region in which the lower sub-alpine is characterized by lodgepole pine, sub-alpine fir, or Engelmann spruce forests, and the foothills and upper foothills are dominated by lodgepole pine.

After intensively managing all areas in 2006 by spot removal of clusters of infested trees, Alberta Agriculture and Forestry designated a region that encompassed our study area as an unmanaged containment zone in 2007 (Ranasinghe et al. 2007), leading to a management free window from 2007 until the collapse of the local outbreak (Fig. 2B). Therefore, any red-attacked tree detected in 2007 by aerial surveyors would have produced a cohort of beetles that would subsequently colonize new host trees that would be detected in 2008. Thus, we were able to use infestations that were detected in 2007 and 2008 to elucidate natural dispersal and attack processes. Because the local outbreak collapsed in 2009, only two unmanaged years were available for model fitting (infestations detected in 2007 and 2008).

For model fitting purposes, we superimposed a grid with square 250 × 250 m (6.25 ha) cells over the study area and summed the number of infested trees within each grid cell. We chose 250 × 250 m grid cells because our tree inventory data (estimates of pine volume on the landscape) were at this resolution.

Tree inventory

Tree inventory data for the Willmore Wilderness Park were unavailable so we obtained pine volume/ha data from Beaudoin et al. (2014) and converted this to an estimate of the number of stems/grid cell in our study area. Pine volume/ha data were spatial raster layers constructed by combining information on the relative proportion of various tree species and the total volume/ha of biomass estimated with Moderate Resolution Imaging Spectroradiometer (MODIS) imagery (Beaudoin et al. 2014). These data were at a spatial resolution of 250 × 250 m (6.25 ha grid cells).

With information on stand age and site productivity, we constructed a tree model to convert data on pine volume/ha to the number of susceptible pine stems/ha in our study area. Most forested areas in the Willmore Wilderness Park that were susceptible were between 60 and 200 years old in 2006 (Graham and Quintilio 2006). However, knowledge of stand age and pine volume/ha was not enough to allow us to determine the number of susceptible pine stems/ha because site productivity varies across the province and will have a large influence on stem counts. To quantify site productivity, we used site index, a measure of site productivity commonly used by forest managers in government and industry (Monserud et al. 2006). Site index quantifies site productivity based on the height of an average tree that is 50 yr old when it's age is measured at breast height (1.3 m). Based on data in Monserud et al. (2006), we assumed that the site index in our study region was between 12 and 15 m at 50 yr breast height age. This corresponds to a medium site as defined by the Alberta Phase 3 Forest Inventory (Alberta Forestry, Lands and Wildlife Department 1985) which has a site index of 14 m at 50 yr breast height age.

Stand age and site index information were used in combination with Alberta Phase 3 Forest Inventory (Alberta Forestry, Lands and Wildlife Department 1985) tables to construct a nonlinear regression to estimate the number of stems/ha that corresponded to each volume/ha (Appendix S1). We only estimated the number of stems/ha that were larger than 10 cm diameter at breast height as mountain

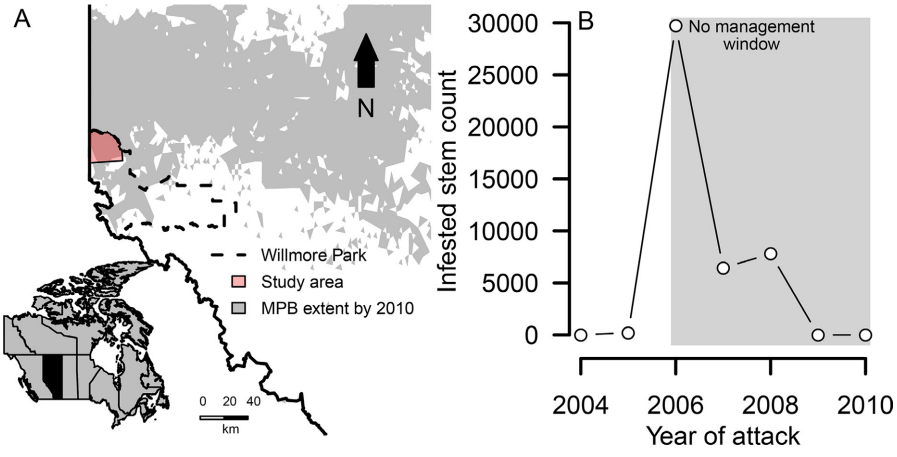

FIG. 2. A map of (A) the study area relative to the extent of mountain pine beetle infestation in Alberta by 2010 (mountain pine beetle infestation extends beyond the northern and eastern edges of the map), and (B) a plot of the progression of the local mountain pine beetle outbreak in the study area from 2004 to 2010. The infested stems turned red and were detected by aerial surveyors one year later (2005–2011).

pine beetles do not usually attack trees of lesser diameter (Safranyik and Carroll 2006). As each grid cell in our tree volume data and in our rasterized infested tree data was 250 × 250 m (6.25 ha), we multiplied the stem/ha estimates by 6.25 to obtain an estimate of the number of stems of diameter greater than 10 cm at 1.3 m in each grid cell. Note that an important assumption of our conversion of densities in the data of Beaudoin et al. (2014) to stem counts is that variability in density, and therefore also in stem counts was due to variation in stand age and not in site quality. Using the data of Beaudoin et al. (2014) in this way, we were able to account for spatial heterogeneity in tree density across the landscape. We were not, however, able to resolve clustering of trees within grid cells in our study area.

Beetle productivity

Managers also collected data on mountain pine beetle productivity within trees in our study area. Surveyors randomly selected 10–20 trees per site, ensuring that mountain pine beetle populations were not disrupted by woodpecker predation. Two samples were collected from the north and south sides near breast height (1.3 m) on each selected tree (four samples total) with a drill fitted with a 10.16 cm (4 inch) diameter hole saw bit. Samples contained a circular bark sample within which mountain pine beetle progeny could be found, as well as a small amount of xylem. Samples were taken back to a laboratory where the total number of live beetle life stages/sample and number of entrance holes were counted. A measure of mountain pine beetle productivity called the *r*-value was then computed by summing the total number of live beetles/tree divided by the total number of entrance holes.

These data were available for spring of 2007 and were, therefore, useful for the parameterization of models that predicted numbers of infested trees attacked in 2007 but detected in 2008. We summarized the *r*-value data by averaging all tree-level *r*-value data collected for the spring of 2007 in our study region (1.33 beetle progeny/attack).

Estimation of the number of adult beetles produced per successfully attacked tree required us to scale beetle productivity statistics per female up to the tree level using estimates and data available in the mountain pine beetle literature (Klein et al. 1978). Raffa and Berryman (1983) estimated that the optimum attack density for beetle productivity in lodgepole pine trees (*Pinus contorta* var. latifolia) is 62 attacks/m at breast height (1.3 m) . However, mountain pine beetle attacks are not distributed uniformly along pine stems (Klein et al. 1978). Rather, attacks are most frequent at approximately 3 m and decrease above and below this height (Klein et al. 1978). Klein et al. (1978) sampled 105 mountain pine beetle attacked trees by dividing their stems into six 1.524 m long sections plus two 0.762 m long sections. Using these data we computed the proportion of attacks that occurred in each section of the stem as well as its bark surface area (data reproduced in Appendix S2: Table S1).

The distribution of diameter classes of attacked trees in our study area was very similar that in the Klein et al. (1978) study (Appendix S2: Fig. S1). Therefore, we computed the total number of attacks that would have occurred in the corresponding section sampled by Klein et al. (1978) assuming that attack density at breast height was 62 attacks/m. We then used data from Klein et al. (1978) on the proportion of attacks in each section to compute the corresponding number of attacks that would likely have occurred in the other tree sections. Using these data we estimated that an average sized tree that was mass-attacked by mountain pine beetles in our study area was attacked 606 times by female mountain pine beetles.

To estimate mountain pine beetle productivity on the tree-level we multiplied 606 by the estimate of within-tree productivity based on the *r*-value data. This multiplication gives an estimate of the total number of beetles produced per successfully attacked tree. However, only female beetles initiate attacks, and sex ratios tend to be skewed (Safranyik and Carroll 2006). Beetles reared in bolts cut from trees in Grande Prairie, Alberta, north of our study areas produced two females for every three beetles (Mory, B, *unpublished data*). Therefore, we multiplied our beetle productivity estimates by two-thirds to obtain an estimate for the number of female beetles produced per successfully attacked tree (606 attacks/tree × 1.33 beetles/attack × 2/3 females/beetles ≈ 537 females/tree).

Models

We derived spatiotemporal models of mountain pine beetle dynamics by modifying the Nicholson–Bailey parasitoid–host models (Nicholson 1933, Nicholson and Bailey 1935) to include aggregation, mass-attack, a critical attack threshold, and beetle dispersal. Due to the inclusion of the critical attack threshold, our modified Nicholson–Bailey models exhibit a strong Allee effect for beetles (the parasitoids). These Nicholson–Bailey-based models are simpler than the most mechanistic mountain pine beetle models in the literature, but nonetheless mechanistically incorporate beetle aggregation and critical attack thresholds created by tree defenses.

Nicholson–Bailey-based model

If P_t is the number of female parasitoids and N_t is the number of hosts in a given area at time t, then the evolution of the Nicholson–Bailey system over time is described by

$$P_{t+1} = cN_t(1 - F(j;m_t)), \tag{1a}$$

$$N_{t+1} = \lambda N_t F(j;m_t), \tag{1b}$$

in which c and λ are geometric growth factors for the parasitoid and host, respectively. More accurately, c

controls the geometric growth of parasitoid females. For most solitary parasitoids, $c = 1$. The function $F(j;m_t)$ is the survival function for the host. Typically $F(j;m_t) = \sum_{i=0}^{j} f(i;m_t = aP_t)$, where $f(i;m_t = aP_t)$ is the Poisson probability mass function that gives the probability of i attacks per host when the mean number of attacks per host is $m_t = aP_t$. The a parameter is the parasitoid attack rate (Hassell 1978), and $j = 0$ is the number of attacks per host that it can sustain and still avoid parasitism in the Nicholson–Bailey model.

Mountain pine beetle attacks are aggregated in some hosts and not in others. A standard way to incorporate aggregation in parasitoid–host models is to assume that $f(i;m_t)$ is a negative binomial probability mass function (May 1978):

$$f(i;m_t) = \left(\frac{k}{k+m_t}\right)^k \frac{\Gamma(k+i)}{i!\Gamma(k)} \left(\frac{m_t}{k+m_t}\right)^i, \qquad (2)$$

in which k is the overdispersion parameter (inversely related to aggregation), m_t is the mean number of attacks per host in generation t.

Mountain pine beetles also differ from parasitoids in that females typically do not oviposit in multiple host trees because the female beetle becomes embedded in the tree during the attack process. Although exceptions occur (Reid 1958), we assume that each female beetle attacks and oviposits in only one host tree. A simple starting assumption is that beetles distribute their attacks evenly over all susceptible hosts in a forested area, Let B_t be the number of attacking female beetles and S_t be the number of susceptible host trees in a given area at time t. We assume that the expected number of attacks per tree is

$$m_t = B_t / S_t. \qquad (3)$$

With aggregation, variability around the expected number of attacks per tree in the stand will be larger than if attacks were randomly distributed. Thus, with aggregation, a few trees will experience mass attack while most will not be attacked or will be attacked infrequently.

In the mountain pine beetle system, attack success is a function of the density of attacking beetles/bark surface area (Raffa and Berryman 1983). When there were 40 attacks/m2 of bark or more, Raffa and Berryman (1983) noted that the defensive capabilities of their study trees were exhausted and they succumbed to attack. When the attack density was below this threshold, trees successfully repelled attacks. By computing an average vulnerable bark surface area per tree, and with knowledge of how beetle attacks are distributed along pine stems (Klein et al. 1978), this 40 attacks/m2 threshold can be scaled up so that it describes the average number of attacks per tree required for tree death. Thus, unlike traditional parasitoid hosts systems a minimum number of attacks per tree that is much larger than one attack per host is required for mountain pine beetles to colonize a host tree and reproduce.

When adjusted to account for aggregation and the critical attack threshold, the survival function for host trees in the mountain pine beetle system becomes

$$F(\phi;m_t) = \sum_{i=0}^{\phi} f(i;m_t). \qquad (4)$$

where $f(i;m_t)$ is given in (Eq. 2) and m_t is given in (Eq. 3). This survival function represents the probability that a susceptible tree is attacked φ or fewer times. An implicit assumption in our model is that any tree that was unsuccessfully mass attacked in a previous generation recovers its full vigor by the next generation. Recasting the negative binomial distribution in terms of the incomplete beta function (Pearson 1968) facilitates simulation and model fitting by eliminating the need to compute large sums (details in Appendix S3). To illustrate how mountain pine beetle attack success probability changes as a function of aggregation (k) and the critical attack threshold (φ) we define the attack function as $1 - F(\phi;m_t)$. As aggregation increases (k decreases), the inflection point in the attack function curve shifts towards zero (Fig. 3).

Using (Eq. 4), we can write the following system that is analogous to (Eq. 1), but which is more representative of the mountain pine beetle:

$$B_{t+1} = cS_t(1 - F(\phi;m_t)), \qquad (5a)$$

$$S_{t+1} = \lambda S_t F(\phi;m_t). \qquad (5b)$$

Mountain pine beetle outbreaks occur on much shorter time scales than are required for tree regrowth and so we assume $\lambda = 1$ (trees do not self-replace).

The survival function described previously (Eq. 4) assumes that the system is closed and therefore no beetles immigrate from outside the study area, an unrealistic assumption for most ecological scenarios. However, it can be modified by making the mean number of attacks depend on the density of immigrating beetles,

$$m_t = \frac{B_t + \zeta_t}{S_t}, \qquad (6)$$

where ζ_t represents the density of female beetles that immigrate in year t.

Integrodifference equation model

Due to localized dispersal, mountain pine beetles as well as their host trees were clustered and not well-mixed or uniformly distributed in space. Thus, the Nicholson–Bailey-based model described in the previous section required a spatial component to be relevant to patterns of mountain pine beetle infestation that occur over large and spatially heterogeneous landscapes. We used integrodifference equations to integrate local mountain pine beetle dispersal and population dynamics. Integrodifference equation models are discrete-time continuous-space

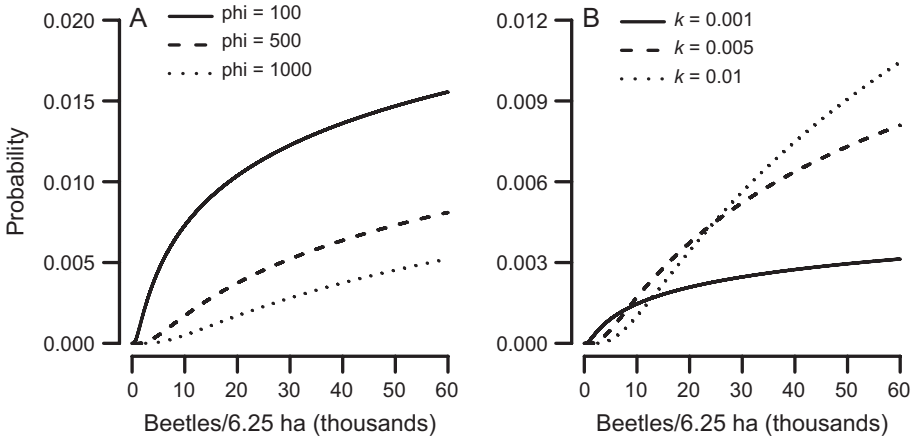

FIG. 3. The attack function $(1-F(S_t,B_t))$, where $F(S_t,B_t)$ is given in (Eq. 4) with varying (A) attack thresholds at which the mountain pine beetle is able to colonize trees (φ) with aggregation held constant ($k = 0.005$) and (B) levels of aggregation (k) where aggregation increases as k decreases, when the attack threshold is constant ($\varphi = 500$). Note the difference in scale in the probability of successful attack along the y-axis between the two figures. In all cases the density of susceptible trees was 3,000 stems/6.25 ha.

models that are suitable for organisms with synchronized dispersal (Kot et al. 1996). Our Nicholson–Bailey-based integrodifference equation was

$$\underbrace{B_t(x)}_{\text{dispersed beetles}} = c\int_\Omega \underbrace{k(x,y)}_{\text{dispersal}} I_t(y)dy, \tag{7a}$$

$$\underbrace{I_{t+1}(x)}_{\text{infested trees}} = S_t(x)\underbrace{\left(1-F(\phi,m_t=(B_t+\zeta_t)/S_t)\right)}_{\text{attack function}}, \tag{7b}$$

$$\underbrace{S_{t+1}(x)}_{\text{susceptible trees}} = S_t(x)-I_{t+1}(x), \tag{7c}$$

where $B_t(x)$ is the density of attacking (female) beetles at location x and generation t, $I_t(x)$ is the density of beetle infested trees, and $S_t(x)$ is the density of susceptible trees. The dispersal kernel, $k(x;y)$, describes the probability density associated with an individual beetle starting at location $y = (y_1,y_2)$ and moving to location $x = (x_1,x_2)$.

To simulate and fit integrodifference equation models to data, we discretized them in space. Thus, our state variables became $B_{g;t}$, $S_{g;t}$, and $I_{g;t}$, in which the index g designates a grid cell in the discretized spatial domain. We used fast Fourier transforms (Singleton 1969) on the discretized spatial domain to efficiently compute the convolution integral (Eq. 7a). The method we used to simulate our integrodifference equation models was based on a tutorial by Jim Powell as well as the appendix of Andersen (1991).[6]

For our model simulations, we used reflecting boundary conditions on all four sides of the spatial domain. No known beetle infested trees were observed near the boundary inside and outside our study area on the west (left), east (right), and south (bottom) edges of our spatial domain. An outbreak similar to the one inside our study area occurred on the north side of our study area. This northern outbreak, however, was managed by Alberta Agriculture and Forestry and so was excluded from the present study. We chose reflecting boundaries because we assumed that the number of beetles dispersing into and out of our study area across the northern boundary was roughly equivalent. Note also that in our model fitting, we excluded observations in areas inside the study area that were managed. As a result, observations within 250 m of the edge of our spatial domain were usually excluded. This exclusion minimized the effect of boundary conditions on maximum likelihood parameter estimates.

[6] http://www.math.usu.edu/powell/wauclass/node1.html

Dispersal models

We incorporated two models of beetle dispersal in the integrodifference equation model described in the previous section. Our first dispersal model assumes that beetles stop flying at a constant rate. The following kernel can be derived from a system of partial differential equations that describes changes in the density of flying and settled beetles over time under the assumption that their flight paths resemble random walks in a two spatial dimensions (Van Kirk 1995):

$$k(x,y) = \frac{\eta^2}{2\pi}\mathcal{K}_0(\eta||x-y||), \tag{8}$$

where $\mathcal{K}_0$ is the modified Bessel function of the second kind and zeroth order. In (Eq. 8) $\eta = \sqrt{(a/D)}$, where a is the constant settling rate and D is the diffusion coefficient. The dispersal kernel describes the probability density associated with individual that starts at location $y = (y_1,y_2)$ and moves to location $x = (x_1,x_2)$. Laboratory flight mill experiments confirm that a constant settling rate accurately describes the stopping rate of mountain

pine beetles flying on flight mills (see Appendix S4: Fig. S1). In reality, beetles that settle will usually land on potential host trees. In (Eq. 8), however, beetle settling does not depend on the presence of host trees. As a result, simulated beetle dispersal will result in some beetles settling in locations that have no susceptible host trees.

An alternative insect flight hypothesis is that insects disperse diffusively and settle instantaneously and synchronously. This can be represented using the Gaussian dispersal kernel

$$k(x,y) = \frac{1}{4\pi D\tau_s}\exp\left(\frac{-(||x-y||^2)}{4D\tau_s}\right), \quad (9)$$

in which D is the diffusion constant and τ_s is the instantaneous settling time. We compared models that featured (Eq. 8) and (Eq. 9) to determine which dispersal hypothesis is more accurate for the mountain pine beetle.

Parameterization of both dispersal models required that we fit one parameter per model. For the diffusion with settling model (Eq. 8), we needed to estimate η, and for the Gaussian dispersal kernel (Eq. 9) we had to estimate the product of the diffusion parameter and the stopping time ($D\tau_s$) as there was no way to estimate them separately.

To estimate the dispersal parameters, we used information from a mountain pine beetle mark–recapture study (Safranyik et al. 1992). In their study Safranyik et al. (1992) found that 93% of beetles were recaptured within 30 m of where they were released in 1982 (Safranyik et al. 1992). In a later trial in 1983 that was part of the same study, only 86% beetles were recaptured within 30 m of where they were released (Safranyik et al. 1992). We used the first statistic to parameterize the models in the current study rather than the second because by 1983 mountain pine beetle had depleted many of the trees in the experimental stands and so the statistic from the second year likely does not reflect dispersal in fully stocked stands (Safranyik et al. 1992). As we had only one parameter to fit for each dispersal model, we computed the empirical cumulative density functions for each kernel with respect to distance and then chose the parameter (η or $D\tau_s$) that made the statistic true (93% of beetles remained within 30 m of release points).

Probabilistic models

In the previous sections we have developed mechanistic mathematical models that describe the spatiotemporal dynamics of the mountain pine beetle. These models predict the expected density of infested stems per grid cell, but to fit them to data, requires that we assume that the infested tree data have some probabilistic distribution. The distribution should be chosen based on an understanding of the nature of the data as well as the biology of the system. The data available for model fitting consisted of aerially surveyed counts of red-attack mountain pine beetle infested trees per 250 × 250 m grid cell.

One appropriate model for the counts of infested trees in a cell is the binomial distribution with a number of trials given by the number of susceptible trees, and the probability of infestation (mortality) given by the attack function in (Eq. 7b). If, however, the count of susceptible trees is also a Poisson random variable with a mean given by the expected number of susceptible trees, then the binomial model for tree infestation becomes a Poisson model with a mean equal to the attack function multiplied by the expected number of susceptible host trees,

$$X_{g,t+1} \sim \text{Poiss}(\mu = S_{g,t}(1 - F(\phi;m_t))). \quad (10)$$

This probabilistic model for counts of infested trees can easily be modified so that it classifies cells as infested or uninfested as follows:

$$\Pr(Y_{g,t+1} = 1) = 1 - \exp(-S_{g,t}(1 - F(\phi;m_t))), \quad (11)$$

in which $Y_{g,t+1}$ is an indicator variable for the presence of mountain pine beetle infested trees and is therefore either a zero (absent) or a one (present).

All of components of integrodifference models of mountain pine beetle dynamics are synthesized in Appendix S5.

Model Fitting, Selection and Assessment

The within-tree beetle productivity parameter (c) was estimated as described in the beetle productivity data section and the dispersal parameters were estimated as described in the section on dispersal models. The remaining three parameters to be estimated for the population dynamics model were the beetle immigration parameter (ζ_t), the aggregation parameter (k), and the critical attack threshold (φ).

To fit the remaining free parameters, we assumed that the expected number of infested trees was given by the discretized version of (Eq. 7b) and the distribution of observations around the expectation was given by the Poisson distribution as described in the probabilistic model section. We then used the Nelder-Mead algorithm (Nelder and Mead 1965) to maximize the likelihood of our mathematical and statistical model. Parameter estimation, however, was difficult as the minimization algorithm frequently found local rather than global minimums of the negative log-likelihood.

To minimize the chances of failing to discover the global minimum negative log-likelihood that corresponded to the maximum likelihood, we performed an exhaustive grid search of the parameter space in which we computed the negative log likelihood for 1.25e5 combinations of the parameters. We chose the parameter set from the 1.25e5 long list of parameter combinations that minimized the negative log-likelihood and then used the Nelder–Mead simplex algorithm (Nelder and Mead 1965) to further minimize the negative log-likelihood starting the minimization algorithm at the optimal parameter set discovered using the grid search.

Model selection and assessment

Because all of our models had the same number of fitted parameters, we selected the best model based on the negative log-likelihood (lower is better) from the integrodifference equation models featuring each of the two dispersal kernels. The negative log-likelihood used in model selection was the same one computed when fitting the parameters as we had no external data to validate our models. We evaluated our best model based its ability to correctly classify grid cells as infested or not infested as well as on it's performance as a predictor of the density of mountain pine beetle infested trees. We assessed the model's ability to predict the density of red-attacked trees by fitting a Poisson generalized linear model to the observed number of infestations as a function of the predictions of the fitted model and computing the pseudo-R^2 statistic for the model (Dobson 2002).

Error analysis

In order to make inferences on the confidence bounds of parameter estimates, it is necessary to have identical and independently distributed errors. Thus, errors should not be highly correlated in space or time. We tested our errors by computing spatial autocorrelation of our negative log-likelihood estimates at each location in space. We then estimated correlograms (variation in the correlation of errors with distance) using nonparametric covariance functions (Bjornstad 2013).

Using an error analysis technique, we propagated uncertainty in parameter estimates to uncertainty in the predictions of the population growth component of our model (Eq. 12). Our method of error analysis follows that of Pacala et al. (1996). During maximum likelihood parameter estimation, in addition to maximum likelihood estimates of parameters, we obtained an estimate of the Hessian matrix. We inverted the negative Hessian matrix to obtain an asymptotic estimate of the covariance matrix. We then sampled from a multivariate normal distribution with means given by our vector of parameter estimates and variance and covariance given by the estimated covariance matrix. Using 1,000 samples from this multivariate normal distribution, we constructed quantile-based 95% confidence intervals around the predictions of (Eq. 12) for each value of Z_t. This method is a numerical equivalent to analytically computing confidence estimates on model predictions using the delta method. An important caveat of these error analyses is that, due to spatial autocorrelation in the errors of our original model, they likely underestimate uncertainty in model predictions.

All simulations and analyses were run using R software (R Core Team 2015) with the Rcpp package (Eddelbuettel and Romain 2011, Eddelbuettel 2013) to speed up computation. We evaluated spatial autocorrelation of errors using the ncf (Bjornstad 2013) package in R and used the raster (Hijmans 2015) package to visualize and manipulate raster files. We used the pROC R package (Robin et al. 2011) to compute ROC curves to evaluate the performance of our best model as a classifier and the rootSolve (Soetaert 2009, Soetaert and Herman 2009) R package to compute the roots of nonlinear difference equations.

Results and Analysis

Our best model based on negative log-likelihood estimates of integrodifference models obtained during model fitting featured the diffusion with settling dispersal kernel (fitted parameters in Table 1). The negative log-likelihood of the integrodifference equation model with a kernel based on diffusion and settling was 13,204 compared to 13,738 for the model that featured the Gaussian kernel.

The integrodifference model with the diffusion and settling kernel fitted the data adequately given the fine resolution of our spatial grid (Fig. 4). Fitted model predictions for the density of beetle infested trees increased with the observed density, and the model explained approximately 29% of the variation in the density of infested trees (Fig. 5A) in addition to accurately predicting the locations of infestations. However, our model did not account for all of the spatial covariation between locations as there was some spatial autocorrelation in model errors over distances of up to 5 km (Fig. 5B).

The accuracy of the model as a predictor of the locations of infestations can be assessed more easily when the model is used to classify cells as infected or uninfected. The area under the curve (AUC) of the receiver operator characteristic curve of the fitted model when it was used to classify observations in the training set was 0.88, which indicates a good fit (Fig. 6). However, two distinct

Table 1. Parameter estimates for the integrodifference equation model with diffusion and settling type dispersal.

Parameter	Significance	Estimate	Units
η	Dispersal parameter	0.677	km
φ	Attack threshold	545 (515, 575)	Attacks
k	Aggregation	3.40e-03 (3.22e-3, 3.57e-3)	Beetles/tree
ζ	Immigration	900 (851, 949)	Beetles
c	Beetle productivity	537	Beetles/tree

Notes: Lower and upper Wald type 95% confidence intervals are included in brackets next to estimates obtained by maximum likelihood estimation. Confidence intervals, however, are likely overly narrow as our model error was spatially auto correlated and therefore, our observations were not independent given our model.

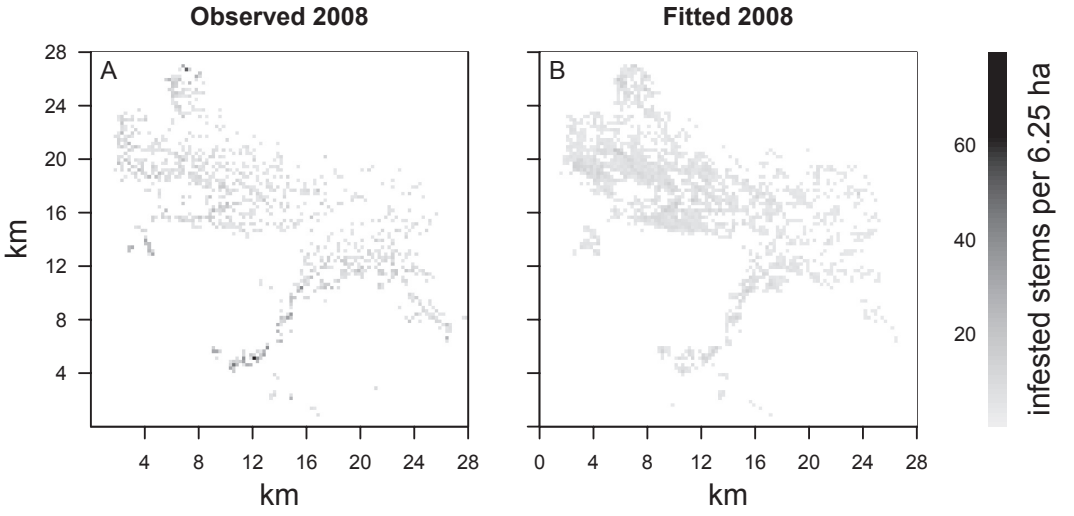

FIG. 4. Maps of (A) observed counts of mountain pine beetle infested trees vs. (B) spatial model fits of modeled counts of mountain pine beetle infested trees. The color bar represents the density of mountain pine beetle infested pine trees (stems/6.25 ha) where 6.25 ha is the size of the grid cells (250 × 250 m) dictated by the resolution of tree inventory data.

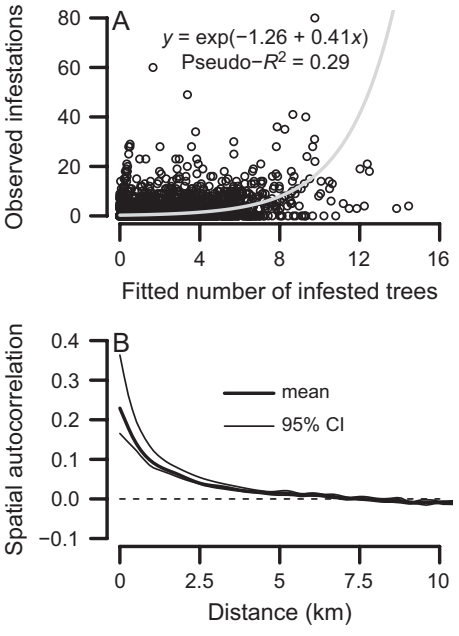

FIG. 5. Model fit assessment plots of (A) observed counts of mountain pine beetle infested pine stems per grid cell vs. estimated numbers of mountain pine beetle infested trees per grid cell based on the fitted model where a Poisson generalized linear model was fitted to enable assessment of model quality using pseudo-R^2, and (B) the estimated spatial autocorrelation of negative log-likelihoods at each grid location in the study area. Estimates of spatial autocorrelation of negative log-likelihoods were obtained using nonparametric covariance functions (Bjornstad 2013).

probability cutoff thresholds for the classifier were evident (vertical lines in Fig. 6). These represent a trade off between model sensitivity (true positive rate) and model specificity (one minus false positive rate). The sensitivity-specificity trade-off is also evident in the classification maps, with the low-specificity threshold (0.045) showing a high number of false positives (Fig. 7A) relative to the high specificity threshold (0.376) map (Fig. 7B).

To better understand the ramifications of the nonlinear population dynamics, we analyzed the difference equation component (Eq. 5) of the integrodifference equation model (Eq. 7). Let $Z_t = B_t/S_t$ be the ratio of beetles to susceptible trees at time t. Thus, (Eq. 5) can be rewritten as a single difference equation

$$Z_{t+1} = \frac{c(1 - F(\phi, m_t = Z_t))}{F(\phi, m_t = Z_t)}, \tag{12}$$

As the system of two coupled difference equations reduces to a single difference equation, the discrete time map is amenable to graphical analysis (Fig. 8A). The population dynamics component of the model predicts population collapse in our study area with no outbreak threshold (solid line in Fig. 8A) because of low within-tree beetle recruitment (r-value). However, assuming that the model correctly represents mountain pine beetle dynamics, we can extrapolate to the situation where beetle recruitment is sufficient to sustain an outbreak (dashed and dotted lines in Fig. 8A). For example, when within tree recruitment is 5.32 beetles produced per female beetle, the Allee threshold is approximately 2.41 (±0.14) beetles per susceptible tree where the number in brackets is the 95% CI based on our error analysis. When within tree recruitment is 6.65 beetles produced per female beetle, the Allee threshold is approximately 1.66 (±0.08) beetles per susceptible tree (Fig. 8A). Thus, increased within tree recruitment results in lower Allee thresholds at the stand level.

By plotting a bifurcation plot as a function of female beetle productivity (Fig. 8B), we can see that the threshold

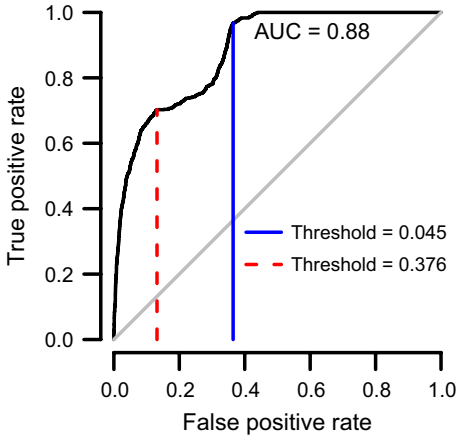

FIG. 6. The Receiver Operating Characteristic (ROC) curve for the best model when used as a classifier (categorizing cells as infested or uninfested). It is produced by varying the threshold probability at which a cell is classified as infested and then computing the true positive and false positive rates. Note that there are two optimum thresholds and selection of one or the other depends on how the optimum is defined. If the optimum is defined as the point along the curve that is closest to the top left corner of the plot, then the optimum probability threshold is 0.376. If the optimum is dictated by the greatest distance between the one to one curve (diagonal) and the ROC curve, then the optimum probability threshold is 0.045.

productivity per female required for eruptive dynamics is approximately 4.79 female beetles produced per attacking female. As female beetle productivity increases beyond this threshold productivity level, the unstable strong Allee threshold decreases and the stable ratio equilibrium (outbreak equilibrium) increases (Fig. 8B).

The meaning of the stable outbreak equilibrium is subtle as without host tree reproduction, no stable coexistence equilibrium can exist because the beetle either goes extinct or it drives its host extinct and then vanishes given that it must kill and colonize hosts to survive. The correct interpretation of the stable outbreak equilibrium for the ratio variable (Z) is elucidated by plotting the phase plane for the system of difference equations (Eq. 5). The stable and unstable outbreak equilibria in Fig. 8B are, in fact, lines on the phase portrait (Fig. 8C). Population trajectories move away from the unstable ratio equilibrium and towards the stable ratio equilibrium if the initial beetle population is above the strong Allee threshold (Fig. 8C). As the trajectory moves parallel to the stable ratio equilibrium both the beetle population and the susceptible tree density approach zero at a constant rate. Thus, the stable outbreak equilibrium results in the extinction of both species in the absence of tree reproduction. If initial population densities are below the strong Allee threshold (below the dashed line in Fig. 8C), then beetle populations go quickly to zero and tree populations persist.

Aggregation reduces the demographic strong Allee threshold as well as the stable outbreak equilibrium (Fig. 9). As aggregation increases (k decreases), the strong Allee threshold approaches zero nearly linearly (Fig. 9) and the strong Allee threshold and the outbreak equilibrium approach one another.

DISCUSSION

The Allee threshold that dictates whether mountain pine beetle infestations outbreak arises because of the interaction between beetle recruitment, aggregation, and tree-level attack thresholds driven by tree defenses. Whether an Allee threshold for mountain pine beetles exists, and the density of beetles per tree above which the Allee threshold is exceeded, depend on beetle recruitment. For example, beetle recruitment of 5.32 beetles per attacking female, produces an Allee threshold of 2.41 (±0.14) beetles per tree. This is lower than the tree-level

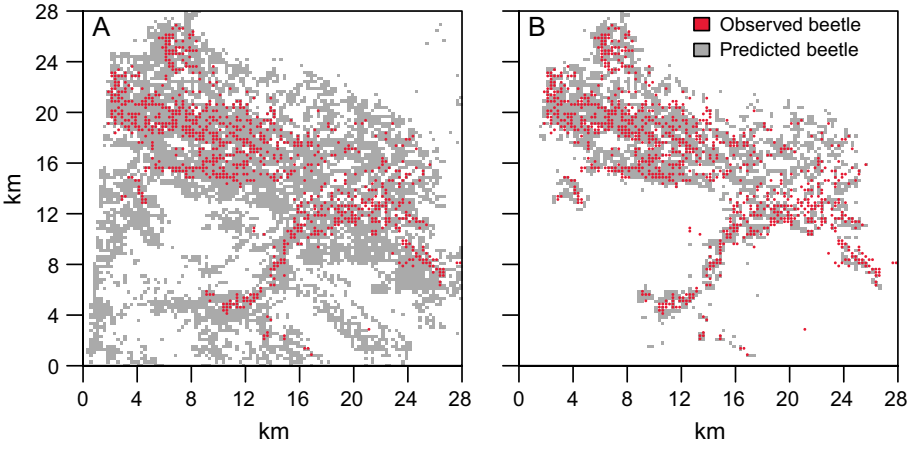

FIG. 7. Maps of (A) observed infested cells vs. predicted infested cells using the best fitted model and a probability threshold of 0.045 and (B) using a probability threshold of 0.376. Each cell is 6.25 ha and the size of the grid cells (250 × 250 m) is dictated by the resolution of tree inventory data.

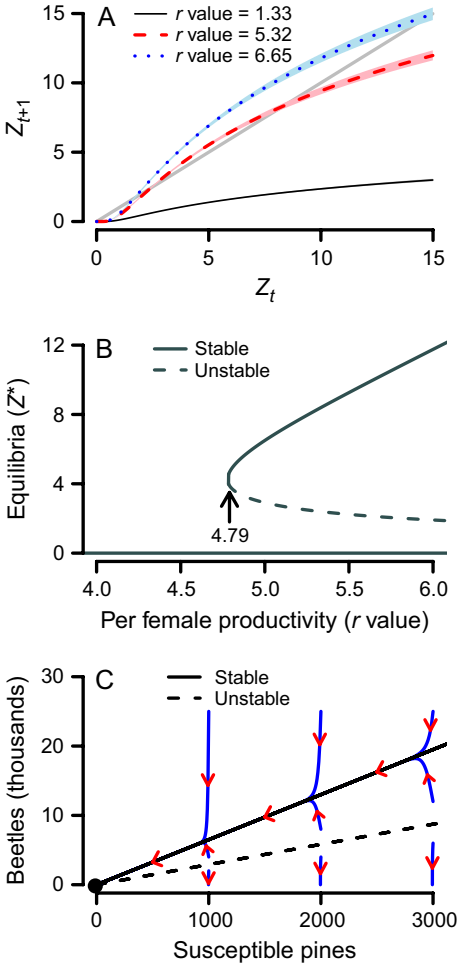

FIG. 8. Dynamics of a nonspatial system of mountain pine beetles and susceptible pine trees (Eq. 5) and (Eq. 12). The discrete time map of (12) when (A) female mountain pine beetle productivity (*r*-value) increases. As female productivity increases an unstable and a stable population equilibrium for the ratio of beetles to susceptible trees (Z) appear. The equilibria (Z^*) occur where the discrete time map curve intersects the one-to-one line shown in grey. The pink and blue shaded regions represent the upper and lower 95% confidence intervals for the discrete-time map. From the bifurcation plot (B), the appearance of stable and unstable equilibria occurs when the per female productivity is approximately 4.79 beetles per female beetle. The dynamics of the system can be succinctly portrayed in a phase diagram (C) on which several hypothetical trajectories for the density of beetles and susceptible host trees are drawn (blue lines). For all analyses, the φ and k parameters were fixed the maximum likelihood estimates given in Table 1. For the simulations shown in the phase diagram, the per female productivity was fixed at five beetles per female and the starting populations of beetle and host trees were varied.

attack threshold of about 545 (±30) beetles per tree precisely because of the ability of the mountain pine beetle to aggregate. Our small k parameter estimate provides evidence for efficient aggregation by pheromone communication in the mountain pine beetle. When beetle densities per host tree are above the strong Allee threshold at the stand level, aggregation enables them to successfully attack host trees even though the beetle to tree ratio at the stand level is below the tree-level attack threshold. Evidently in a stand with only one susceptible tree, this strong Allee threshold will not be applicable, as four beetles cannot overcome a well-defended host. Our results apply to stands with a minimum of a few hundred susceptible host trees per 6.25 ha.

Model selection indicated that the diffusion and constant settling hypothesis better reflected beetle dispersal patterns in our data than the diffusion and instantaneous settling hypothesis embodied in the Gaussian kernel. Heavilin and Powell (2008) found that for the mountain pine beetle, the Gaussian dispersal kernel outperformed the exponential dispersal kernel in two spatial dimensions. The difference between our diffusion with settling kernel and the exponential kernel of Heavilin and Powell (2008) is that the latter assumes directed rather than diffusive movement. Turchin and Thoeny (1993) derived a dispersal kernel for the southern pine beetle (*Dendroctonus frontalis* Zimmermann) that is similar to our diffusion and settling kernel. Like our kernel, the derivation of Turchin and Thoeny (1993) is based on a partial differential equation model of diffusion and constant settling. Unlike our version of the diffusion with settling kernel, which assumes settled beetles attack trees, Turchin and Thoeny (1993) assumed mortality of settled beetles.

In this study we have focused on the interaction between aggregation and Allee thresholds. Although it is difficult to separate aggregation from dispersal, we have done so by assuming that aggregation occurs at a smaller spatial scale than that of local dispersal. Most mountain pine beetles dispersing under the canopy appear to disperse less than 30–50 m (Safranyik et al. 1992) and so aggregative behavior would likely occur at spatial scales much smaller than our grid cell (250 × 250 m). Thus, we

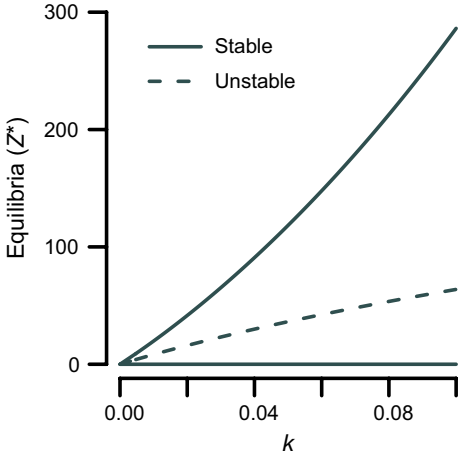

FIG. 9. The effect of aggregation on the demographic strong Allee threshold. As aggregation increases (k decreases), the strong Allee threshold decreases, and fewer initial beetles are needed to cause an outbreak. The plot is shown for female productivity fixed at five beetles per female and the φ parameter fixed at its maximum likelihood estimate given in Table 1.

represent the distribution of beetles within grid cells using a spatially implicit model that features the negative binomial probability mass function (Eq. 2). Clustering in beetles results in clustering of infested trees as not all trees have the same probability of being mass attacked. Assuming, as we have done, that aggregation occurs only within grid cells, however, would be problematic if the resolution of our model were increased (decreased grid cell size) because our estimate of aggregation (k) depends on the spatial scale of grid cells.

In the dispersal model of Powell and Bentz (2014), beetles are more likely to disperse from an area when local host density is low. Unlike in our models, aggregation is a consequence of beetle dispersal in their model. As we could not resolve the spatial clustering of trees within grid cells, we were unable to test the hypothesis that beetles aggregate in areas of high host density (Powell and Bentz 2014). The present study did incorporate spatial heterogeneity in the density of host trees from one grid cell to another but we assumed that this variation was due to variation in stand age. When stands are of different age, high density can be an indicator of young stands which are initially dense before they reach the self-thinning stage of stand development and become susceptible to mountain pine beetle attack (Anhold and Jenkins 1987). For this reason, stands of intermediate density have been found to be more susceptible to mountain pine beetle damage than stands of high density (Anhold and Jenkins 1987). Assuming that the mountain pine beetles move towards the densest aggregations of trees may be risky when applied across the different aged stands in the present study.

Aggregation in the mountain pine beetle system is more complex than the simple representation in our models. Attacking female beetles release aggregation pheromones until the host tree succumbs to attack, whereupon they switch to anti-aggregation pheromones to prevent overcrowding (Hunt et al. 1989, Hunt and Borden 1990, Lindgren and Miller 2002). Anti-aggregation pheromones encourage beetles to attack trees other than those that have already been successfully mass-attacked (Hunt et al. 1989). Thus, when population densities are high, beetles will tend to be less aggregated than when populations densities are low as a (Conn et al. 1983, Borden et al. 1987).

Aggregation levels in the mountain pine beetle depend not only on beetle density, but also on the phase of the outbreak (Safranyik and Carroll 2006, Boone et al. 2011). Safranyik and Carroll (2006) categorized beetle populations into four regimes according to their behavior. Mountain pine beetle population in their endemic phase attack primarily weakened hosts (Safranyik and Carroll 2006). Populations in the incipient-epidemic phase begin to colonize more vigorous hosts (Safranyik and Carroll 2006, Boone et al. 2011). It is during the transition from endemic and incipient-epidemic stages that aggregation is the most critical for the growth of mountain pine beetle populations because population densities tend to be low compared to in the epidemic stage. In the epidemic stage, the mountain pine beetle population outbreaks beetle will focus their attacks on the most vigorous trees stands which also tend to be the most nutritious (Safranyik and Carroll 2006). Finally in the post-epidemic phase, populations collapse due to host depletion or inclement weather. The mountain pine beetle population that generated the data used in this study was in the epidemic stage, but it was transitioning to the post-epidemic phase. Thus, the level of aggregation given by the k parameter that we measured in our study was for an epidemic mountain pine beetle population.

There has been recent interest in the possibility of bivoltinism as a result of climate change in bark beetles that are typically univoltine (Jönsson et al. 2009, Bentz and Powell 2014). A weakness of the integrodifference equation framework for modeling insect dynamics under climate change is that it is difficult to incorporate temperature-dependent variation in the timing of development and dispersal stages. This difficulty was overcome by Powell and Bentz (2014) using a temperature-dependent continuous-time model of mountain pine beetle dispersal and development. As the focus of our study was on the interaction of aggregation and Allee effects created by tree defenses, our model does not account for variation in beetle emergence in response to temperature. Because synchronization in the life cycles in organisms subject to Allee thresholds (Friedenberg et al. 2007) can create population peaks and troughs, aggregation likely plays an important role in enabling population persistence in spite of low population densities that occur between population cycles. Therefore, future studies that account for population phenology and aggregation in the face of Allee effects are needed.

Below a critical per female productivity level (approximately 4.75 beetles produced per attack in this study), outbreak dynamics are impossible and population collapse is inevitable. As a result, when within-tree beetle productivity is low, managers can safely prioritize stands where beetle productivity is higher. Prioritizing in this way will minimize the wasteful management of low productivity mountain pine beetle populations that would collapse on their own even in the absence of management. The exact level of female beetle productivity within hosts at which it is safe to do nothing, however, is uncertain as we have fitted our model to a single pair of years in a small study area, and all of the parameters in our model likely vary from year to year. Thus, using mountain pine beetle productivity within trees to triage infested stands is preferable to basing management decisions on a hard mountain pine beetle productivity cut-off.

Aggregation was an integral component of Allee's thinking about Allee effects (Allee 1931) because organisms whose fitness suffers when their densities are low generally evolve characteristics that enable them to aggregate (Stephens et al. 1999, Stephens and Sutherland 1999, Wertheim , et al. 2002, 2005, Gascoigne et al. 2009). In gregarious parasitoid host systems, for example, the immune system of the host sometimes encapsulates and

incapacitates parasitoid eggs when their numbers are low (Ikawa and Okabe 1985, Takagi 1985). This incentivises superparasitism (Takagi 1985), in which hosts are repeatedly parasitized by the same species of parasitoid. In the mountain pine beetle system, the defensive capacities of host trees are analogous to the immune defenses of the larval hosts of gregarious parasitoids. In organisms, such as these, that are impacted by an Allee effect at the individual level, it is critical to consider how aggregation may change the way in which the Allee effect is expressed when scaled up to the population level.

Acknowledgments

We thank two anonymous reviewers for comments that improved our presentation and discussion of this work. We thank Nadir Erbilgin for commenting on an early draft. This research was supported by a grant to B. J. Cooke, M. A. Lewis, and M. L. Evenden from the Natural Science and Engineering Research Council of Canada (grant no. NET GP 434810-12) to the TRIA Network, with contributions from Alberta Agriculture and Forestry, Foothills Research Institute, Manitoba Conservation and Water Stewardship, Natural Resources Canada-Canadian Forest Service, Northwest Territories Environment and Natural Resources, Ontario Ministry of Natural Resources and Forestry, Saskatchewan Ministry of Environment, West Fraser and Weyerhaeuser. M. A. Lewis is also grateful for support through NSERC and the Canada Research Chair Program.

Literature Cited

Allee, W. C. 1931. Animal aggregations. A study in general sociology. The University of Chicago Press, Chicago.

Andersen, M. 1991. Properties of some density-dependent integrodifference equation population models. Mathematical Biosciences 104:135–157.

Anhold, J. A., and M. J. Jenkins. 1987. Potential mountain pine beetle (coleoptera: Scolytidae) attack of lodgepole pine as described by stand density index. Environmental Entomology 16:738–742.

Alberta Forestry, Lands and Wildlife Department. 1985. Alberta Phase 3 Forest Inventory. Technical report, Alberta Sustainable Resource Development.

Beaudoin, A., P. Y. Bernier, L. Guindon, P. Villemaire, X. J. Guo, G. Stinson, T. Bergeron, S. Magnussen, and R. J. Hall. 2014. Mapping attributes of Canada's forests at moderate resolution through kNN and MODIS imagery. Canadian Journal of Forest Research 44:521–532.

Bentz, B. J., and J. A. Powell. 2014. Mountain pine beetle seasonal timing and constraints to bivoltinism. The American Naturalist 184:787–796.

Biesinger, Z., J. Powell, B. Bentz, and J. Logan. 2000. Direct and indirect parametrization of a localized model for the mountain pine beetle—lodgepole pine system. Ecological Modelling 129:273–296.

Bjornstad, O. N. 2013. ncf: spatial nonparametric covariance functions. R package version 1.1-5.

Boone, C. K., B. H. Aukema, J. Bohlmann, A. L. Carroll, and K. F. Raffa. 2011. Efficacy of tree defense physiology varies with bark beetle population density: a basis for positive feedback in eruptive species. Canadian Journal of Forest Research-Revue Canadienne de Recherche Forestiere 41: 1174–1188.

Borden, J. H., L. C. Ryker, L. J. Chong, H. D. Pierce, B. D. Johnston, and A. C. Oehlschlager. 1987. Response of the mountain pine beetle, *Dendroctonus ponderosae* Hopkins (Coleoptera-Scolytidae) to 5 semiochemicals in British Columbia lodgepole pine forests. Canadian Journal of Forest Research-Revue Canadienne de Recherche Forestiere 17:118–128.

Conn, J. E., J. H. Borden, B. E. Scott, L. M. Friskie, H. D. Pierce Jr., and A. C. Oehlschlager. 1983. Semiochemicals for the mountain pine beetle, *Dendroctonus ponderosae* (Coleoptera: Scolytidae) in British Columbia: field trapping studies. Canadian Journal of Forest Research 13:320–324.

Courchamp, F., L. Berec, and J. Gascoigne. 2008. Allee effects in ecology and conservation. Oxford University Press, New York, New York, USA.

Dobson, A. J. 2002. Introduction to generalized linear models. Chapman & Hall/CRC Press, Boca Raton, Florida, USA.

Eddelbuettel, D. 2013. Seamless R and C++ integration with Rcpp. Springer, New York, New York, USA.

Eddelbuettel, D., and F. Romain. 2011. Rcpp: seamless R and C++ integration. Journal of Statistical Software 40:1–18.

Friedenberg, N. A., J. A. Powell, and M. P. Ayres. 2007. Synchrony's double edge: transient dynamics and the allee effect in stage structured populations. Ecology Letters 10:564–573.

Gascoigne, J., L. Berec, S. Gregory, and F. Courchamp. 2009. Dangerously few liaisons: a review of mate-finding Allee effects. Population Ecology 51:355–372.

Graham, L., and K. Quintilio. 2006. Willmore Wilderness Park Fire Management Plan. Technical report, Alberta Community Development and Alberta Environment and Sustainable Resource Development.

Hassell, M. P. 1978. The dynamics of predator-prey systems. Princeton University Press, Princeton, New Jersey, USA.

Heavilin, J., and J. Powell. 2008. A novel method of fitting spatio-temporal models to data, with applications to the dynamics of mountain pine beetles. Natural Resource Modeling 21:489–524.

Hijmans, R. J. 2015. raster: Geographic Data Analysis and Modeling. R package version 2.4-18.

Hunt, D. W. A., and J. H. Borden. 1990. Conversion of verbenols to verbenone by yeasts isolated from *Dendroctonus ponderosae* (Coleoptera, Scolytidae). Journal of Chemical Ecology 16:1385–1397.

Hunt, D. W. A., J. H. Borden, B. S. Lindgren, and G. Gries. 1989. The role of autoxidation of alpha-pinene in the production of pheromones of *Dendroctonus ponderosae* (Coleoptera, Scolytidae). Canadian Journal of Forest Research-Revue Canadienne de Recherche Forestiere 19:1275–1282.

Ikawa, T., and H. Okabe. 1985. Regulation of egg number per host to maximize the reproductive success in the gregarious parasitoid Apenteles glomeratus L (Hymenoptera, Braconidae). Applied Entomology and Zoology 20:331–339.

Jackson, P. L., D. Straussfogel, B. S. Lindgren, S. Mitchell, and B. Murphy. 2008. Radar observation and aerial capture of mountain pine beetle, *Dendroctonus ponderosae* Hopk. (Coleoptera: Scolytidae) in flight above the forest canopy. Canadian Journal of Forest Research-Revue Canadienne de Recherche Forestiere 38:2313–2327.

Jönsson, A., G. Appelberg, S. Harding, and L. Bärring. 2009. Spatio-temporal impact of climate change on the activity and voltinism of the spruce bark beetle, ips typographus. Global Change Biology 15:486–499.

Klein, W. H., D. L. Parker, and C. E. Jensen. 1978. Attack, emergence, and stand depletion trends of the Mountain Pine Beetle in a lodgepole pine stand during an outbreak. Environmental Entomology 7:732–737.

Kot, M., M. A. Lewis, and P. Van Den Driessche. 1996. Dispersal data and the spread of invading organisms. Ecology 77:2027–2042.

Liebhold, A. M., and P. C. Tobin. 2008. Population ecology of insect invasions and their management. Annual Review of Entomology 53:387–408.

Lindgren, B. S., and D. R. Miller. 2002. Effect of verbenone on five species of bark beetles (Coleoptera: Scolytidae) in lodgepole pine forests. Environmental Entomology 31:759–765.

May, R. M. 1978. Host-parasitoid systems in patchy environments: a phenomenological model. Journal of Animal Ecology 47:833–843.

Monserud, R. A., S. Huang, and Y. Yang. 2006. Predicting lodgepole pine site index from climatic parameters in Alberta. Forestry Chronicle 82:562–571.

Nelder, J. A., and R. Mead. 1965. A simplex method for function minimization. Computer Journal 7:308–313.

Nicholson, A. J. 1933. The balance of animal populations. Journal of Animal Ecology 2:132–178.

Nicholson, A. J., and V. A. Bailey. 1935. The balance of animal populations-Part I. Proceedings of the Zoological Society of London 105:551–598.

Pacala, S. W., C. D. Canham, J. Saponara, J. A. Silander Jr., R. K. Kobe, and E. Ribbens. 1996. Forest models defined by field measurements: estimation, error analysis and dynamics. Ecological Monographs 66:1–43.

Pearson, K. 1968. Tables of the incomplete beta function. Cambridge University Press, New York, New York, USA.

Powell, J. A., and B. J. Bentz. 2014. Phenology and density-dependent dispersal predict patterns of mountain pine beetle (*Dendroctonus ponderosae*) impact. Ecological Modelling 273:173–185.

R Core Team. 2015. R: a language and environment for statistical computing. R Foundation for Statistical Computing, Vienna, Austria. https://www.r-project.org/

Raffa, K. F., and A. A. Berryman. 1983. The role of host plant resistance in the colonization behavior and ecology of bark beetles (Coleoptera: Scolytidae). Ecological Monographs 53:27–49.

Ranasinghe, S., et al. 2007. Annual Report—Forest Health in Alberta. Technical report, Alberta Environment and Sustainable Resource Development.

Reid, R. W. 1958. The behaviour of the mountain pine beetle Dendroctonus monticolae hopk., during mating, egg laying, and gallery construction. Canadian Entomologist 90:505–509.

Robin, X., N. Turck, A. Hainard, N. Tiberti, F. Lisacek, J.-C. Sanchez, and M. Mller. 2011. proc: an open-source package for r and s+ to analyze and compare roc curves. BMC Bioinformatics 12:77.

Robinet, C., D. R. Lance, K. W. Thorpe, K. S. Onufrieva, P. C. Tobin, and A. M. Liebhold. 2008. Dispersion in time and space affect mating success and Allee effects in invading gypsy moth populations. Journal of Animal Ecology 77:966–973.

Safranyik, L., and A. Carroll. 2006. The biology and epidemiology of the mountain pine beetle in lodgepole pine forests. Pages 3–66 *in* Les Safranyik and Bill Wilson, editors. The Mountain Pine Beetle: a synthesis of its biology, management and impacts on lodgepole pine. Canadian Forest Service, Victoria, BC.

Safranyik, L., D. Linton, R. Silversides, and L. McMullen. 1992. Dispersal of released mountain pine beetles under the canopy of a mature lodgepole pine stand. Journal of Applied Entomology 113:441–450.

Singleton, R. 1969. An algorithm for computing the mixed radix fast Fourier transform. IEEE Transactions on Audio and Electroacoustics 17:93–103.

Soetaert, K. 2009. rootSolve: nonlinear root finding, equilibrium and steady-state analysis of ordinary differential equations. R package version 1.6.

Soetaert, K., and P. M. J. Herman. 2009. A practical guide to ecological modelling using R as a simulation platform. Springer, Berlin.

Stephens, P., and W. Sutherland. 1999. Consequences of the Allee effect for behaviour, ecology and conservation. Trends in Ecology & Evolution 14:401–405.

Stephens, P. A., W. J. Sutherland, and R. P. Freckleton. 1999. What is the Allee effect? Oikos 87:185–190.

Strohm, S., R. C. Tyson, and J. A. Powell. 2013. Pattern formation in a model for mountain Pine Beetle dispersal: linking model predictions to data. Bulletin of Mathematical Biology 75:1778–1797.

Takagi, M. 1985. The reproductive strategy of the gregarious parasitoid *Pteromalus puparum* (Hymenoptera, Pteromalidae) 1. Optimal number of eggs in a single host. Oecologia 68:1–6.

Taylor, C., and A. Hastings. 2005. Allee effects in biological invasions. Ecology Letters 8:895–908.

Tobin, P. C., L. Berec, and A. M. Liebhold. 2011. Exploiting Allee effects for managing biological invasions. Ecology Letters 14:615–624.

Turchin, P., and W. T. Thoeny. 1993. Quantifying dispersal of southern pine beetles with mark-recapture experiments and a diffusion model. Ecological Applications 3:187–198.

Van Kirk, R. W. 1995. Integrodigerence models of biological growth and dispersal. Dissertation. University of Utah , Salt Lake City, Utah, USA.

Wertheim, B., J. Marchais, L. E. M. Vet, and M. Dicke. 2002. Allee effect in larval resource exploitation in Drosophila: an interaction among density of adults, larvae, and microorganisms. Ecological Entomology 27:608–617.

Wertheim, B., E.-J. A. van Baalen, M. Dicke, and L. E. M. Vet. 2005. Pheromone-mediated aggregation in nonsocial arthropods: an evolutionary ecological perspective. Annual Review of Entomology 50:321–346.

Supporting Information

Additional supporting information may be found in the online version of this article at http://onlinelibrary.wiley.com/doi/10.1890/14-1404/full

Data Accessibility

The code used to simulate our model and fit its parameters is included in the online supporting information (Data S1 IDEfit1.R) along with a metadata file that provides details on code implementation (Metadata S1). Data associated with this manuscript have been deposited in Dryad: http://dx.doi.org/10.5061/dryad.r8t33